

# Vortex $\gamma$ photon generation via spin-to-orbital angular momentum transfer in nonlinear Compton scattering

Mamutjan Ababekri,<sup>1</sup> Ren-Tong Guo,<sup>1</sup> Feng Wan,<sup>1,\*</sup> B. Qiao,<sup>2</sup> Zhongpeng Li,<sup>1</sup> Chong Lv,<sup>3</sup> Bo Zhang,<sup>4</sup> Weimin Zhou,<sup>4</sup> Yuqiu Gu,<sup>4</sup> and Jian-Xing Li<sup>1,†</sup>

<sup>1</sup>Ministry of Education Key Laboratory for Nonequilibrium Synthesis and Modulation of Condensed Matter, Shaanxi Province Key Laboratory of Quantum Information and Quantum Optoelectronic Devices,

School of Physics, Xi'an Jiaotong University, Xi'an 710049, China

<sup>2</sup>Center for Applied Physics and Technology, HEDPS and SKLNPT,

School of Physics, Peking University, Beijing 100871, China

<sup>3</sup>Department of Nuclear Physics, China Institute of Atomic Energy, P. O. Box 275(7), Beijing 102413, China

<sup>4</sup>Key laboratory of plasma physics, Research center of laser fusion,

China academy of engineering physics, 621900, Mianshan Rd 64#, Mianyang, Sichuan, China

(Dated: July 21, 2023)

Vortex  $\gamma$  photons with intrinsic orbital angular momenta (OAM) possess a wealth of applications in various fields, e.g., strong-laser, nuclear, particle and astro-physics, yet their generation remains unsettled. In this work, we investigate the generation of vortex  $\gamma$  photons via nonlinear Compton scattering of ultrarelativistic electrons in a circularly polarized laser pulse. We develop a quantum electrodynamics scattering theory that explicitly addresses the multiphoton absorption and the angular momentum conservation. We find that, emitted  $\gamma$  photons possess intrinsic OAM as a consequence of spin-to-orbital angular momentum transfer, and they are in a mixed state of different OAM modes due to the finite pulse shape of the laser. Moreover, the nonlinear Breit-Wheeler scattering of the vortex  $\gamma$  photon in a strong laser can reveal the phase structures of the vortex  $\gamma$  photons. Our findings emphasize the special role played by the intense laser regarding both generation and detection of vortex  $\gamma$  photons, and call for further investigations.

Vortex photons are described by wave functions with helical phases and carry intrinsic orbital angular momenta (OAM) along the propagation direction [1, 2]. Light beams with OAM have significant applications in various fields including optical manipulation [3, 4], quantum optics [5, 6], imaging [7, 8], etc. Due to their new degree of freedom, high energy vortex photons bring an alternative for doing spin physics and promise to shed new light on nuclear and particle physics related researches [9, 10]. Experimental opportunities brought by vortex photons are studied in their collisions with ion beams regarding the existing and future physics programs [11–14]. Vortex photons are also shown to reveal various quantum electrodynamics (QED) effects in [15–18]. Currently, vortex photons from visible to X-ray regimes have been generated utilizing optical mode conversion techniques, high harmonic generation or coherent radiation in helical undulators and laser facilities [19–23]. However, the generation of vortex  $\gamma$  photons still remains a challenge, where most of the studies consider Compton scattering to attain high energy and OAM [24–28].

Ultraintense and ultrashort laser pulses [29–31] have been demonstrated to generate high energy  $\gamma$  photon beams via nonlinear Compton scattering (NCS) [32–35]. The spin angular momentum (SAM) properties of emitted  $\gamma$  photons are revealed in theoretical investigations from moderate to ultraintense regimes [36–38]. The generated  $\gamma$  ray beams are shown to carry OAM as the collective effect of the mechanical OAM of the individual photon defined by  $\mathbf{L} = \mathbf{r} \times \mathbf{p}$  [39, 40]. Although these studies have inspired rich mechanisms for the generation of vortex beams with collective OAM in laser-plasma

interactions [41–46], the intrinsic OAM carried by these photons is still missing from the picture. Most of these studies consider vortex lasers and view the angular momentum transfer relation during NCS as the conversion from intrinsic SAM and OAM of laser photons to the mechanical OAM of final particles. On the other hand, investigations for the charged particle radiation in laser or undulator fields have identified that photons in the radiation field carry intrinsic OAM [47–49]. Recently, this is demonstrated in the QED framework for undulators by investigating NCS in the circularly polarized (CP) monochromatic plane wave field [50]. However, strong lasers are achieved by temporal compression, and the resulting finite pulse shape drastically alters the harmonic contents of the NCS spectra affecting angular momentum properties of radiated  $\gamma$  photons [37, 51]. Furthermore, under realistic intense lasers, the radiated vortex  $\gamma$  photon beam may no longer be recognized as a coherent vortex state with definite polarization and total angular momentum (TAM) [24, 52] as is assumed in the semiclassical [28] and QED [50] studies. The core problem resides in addressing the QED nature of both high energy radiation and the formation of vortex states in more realistic strong laser pulses.

During NCS, each radiation event turns multiple low energy laser photons into a single high energy final photon such that angular momentum transfer relation cannot be addressed if one only considers SAM. Unfortunately, the standard QED treatment of the radiation based on NCS theory mostly investigates the spin as the only internal degree of freedom affecting the process [53, 54]. Thus, the theory fails to grasp the angular momentum conservation property of radiation events when the system respects rotational invariance which could be the case in CP laser fields. Moreover, as the radiation under rotational symmetry could be realized in upcoming intense laser-based

\* wanfeng@xjtu.edu.cn

† jianxing@xjtu.edu.cn

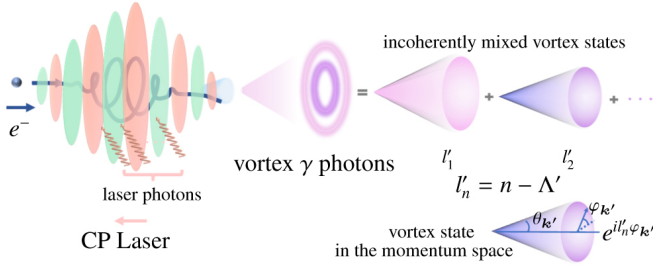


FIG. 1. Generation of vortex  $\gamma$  photons with intrinsic OAM during NCS of the ultrarelativistic energy electron in the CP laser pulse. The intrinsic OAM of the vortex  $\gamma$  photon is  $l'_n = n - \Lambda'$ , where  $n$  labels the corresponding harmonics and  $\Lambda'$  is the  $\gamma$  photon spin. The vortex state is represented by a cone in the momentum space with the polar angle  $\theta_{k'}$  and the azimuth angle  $\varphi_{k'}$  of the momentum vector  $\mathbf{k}'$ .

experiments [55–57], the vortex nature of the radiation calls for detailed investigations in the understanding of strong-field QED processes involving  $\gamma$  photons.

In this Letter, we investigate the generation of vortex  $\gamma$  photons with intrinsic OAM during NCS in an intense CP laser pulse. We develop a scattering theory in the Furry picture of strong-field QED, where multiphoton absorption and angular momentum conservation are explicitly addressed by performing harmonic expansion and employing spin eigenfunctions. The collision geometry is presented in Fig. 1, where an electron propagates along the  $z$ -direction and collides with a counter-propagating CP laser pulse. The wave function of the emitted  $\gamma$  photon possesses the phase vorticity, which encodes spin-to-orbital angular momentum transfer during multiphoton absorption, and displays the desired spiral form indicating the intrinsic OAM carried by the photon [see Eqs. (2) and (3)]. The finite laser pulse would introduce multiple OAM modes into the  $\gamma$  photon with definite energy and polarization due to the ponderomotive broadening of harmonics (see Fig. 2). We point out that, vortex  $\gamma$  photons generated in strong lasers are composed of incoherent mixed states of various vortex eigenmodes (see Figs. 3 and 4). Furthermore, the nonlinear Breit-Wheeler (NLBW) scattering of the vortex  $\gamma$  photons in an intense laser could reveal their phase structures and can be used to measure the vorticity of  $\gamma$  photons (see Fig. 5). Throughout, natural units are used ( $\hbar = c = 1$ , where  $\hbar$  is the Planck constant and  $c$  is the speed of light in vacuum), and the fine structure constant is  $\alpha = \frac{e^2}{4\pi} \approx \frac{1}{137}$  where  $e$  is the electron charge.

We first introduce our theoretical method and present analytical results to reveal the vortex nature of the  $\gamma$  photon and its radiation property. The laser pulse is modeled by a CP background field  $A^\mu(\phi) = \frac{a}{\sqrt{2}}(e^{-i\phi}\epsilon_+^\mu + e^{i\phi}\epsilon_-^\mu)g(\phi)$ , where the laser phase  $\phi = kx$ ,  $\epsilon_\pm^\mu = \frac{1}{\sqrt{2}}(0, 1, \pm i, 0)^T$ ,  $g(\phi)$  is the temporal pulse shape function and  $a = \frac{m_e}{e}\xi$  with the dimensionless parameter  $\xi$  related to the laser intensity via  $\xi \approx \sqrt{7.3 \times 10^{-19} I [\text{W/cm}^2] \lambda_0^2 [\mu\text{m}]}$  and the electron mass  $m_e$ . The momentum 4-vectors for incoming electron, laser field, outgoing electron and emitted photon are  $p = (\varepsilon, 0, 0, p_z)$ ,  $k = (\omega, 0, 0, -\omega)$ ,  $p' = (\varepsilon', \mathbf{p}')$  and  $k' = (\omega', \mathbf{k}')$ , respectively, with corresponding angles  $\theta_{p',k'}$ ,  $\varphi_{p',k'}$ . In order to explore

the angular momentum transfer relation during multiphoton absorption process, we turn the scattering amplitude into a sum over harmonics and keep track of the azimuthal angle dependency explicitly. The former is achieved by employing the slowly varying laser pulse envelope approximation ( $N_{\text{cycle}} \gg 1$ ) [58], while the latter by expanding the final state photon polarization vector and the electron bi-spinors with eigenfunctions of the spin operators [10]. The final form of the NCS  $S$ -matrix element is written as:

$$S_{fi} = \mathcal{N}_{\text{NCS}} \frac{(2\pi)^3}{\omega} \delta^3(\mathbf{p} + s_0 \mathbf{k} - \mathbf{p}' - \mathbf{k}') \sum_n e^{i(n+\lambda-\lambda')\varphi_{p'}} \mathcal{M}_n(s_0), \quad (1)$$

where  $\mathcal{N}_{\text{NCS}} = \frac{-ie}{\sqrt{8\epsilon\epsilon'\omega'}}$ ,  $\lambda$  and  $\lambda'$  are the initial and final electron spins, respectively, and the expression for the amplitude  $\mathcal{M}_n(s_0)$  is given in the Supplemental Material [59]. Note that  $s_0 = \frac{\varepsilon' + \omega' - \varepsilon}{\omega}$  is a continuous number and could be interpreted as the laser photon absorption number, while the integer-valued  $n$  labels the harmonics.

The wave function of the radiated  $\gamma$  photon is related to the final state electron via the  $S$ -matrix element [50, 59–62]. Due to the axial symmetry of the system, the radiation dynamics is azimuth angle independent. Besides, the final electron phase is normally inaccessible in the experiment. These features could be reflected by a final electron wave packet  $\int \frac{d^2\mathbf{p}'_\perp}{(2\pi)^2} \sqrt{\frac{2\pi}{\omega'}} \delta(p'_\perp - \kappa') |\mathbf{p}', \lambda'\rangle$  [59], and one obtains the wave function of the radiated  $\gamma$  photon in the momentum space:

$$\mathcal{A}_{k',\Lambda'} = \mathcal{N}_{\text{NCS}} \frac{(2\pi)^{3/2}}{\omega} \delta(p_z + s_0 k_z - p'_z - k'_z) \frac{1}{\sqrt{k'_\perp}} \delta(k'_\perp - p'_\perp) \times \sum_{n,\sigma_{\Lambda'}} (-1)^{m'_n} e^{i(m'_n - \sigma_{\Lambda'})\varphi_{k'}} d^1_{\sigma_{\Lambda'},\Lambda'}(\theta_{k'}) \chi_{\sigma_{\Lambda'}} \mathcal{M}_n(s_0), \quad (2)$$

where  $m'_n = n + \lambda - \lambda'$ ,  $d^1_{\sigma_{\Lambda'},\Lambda'}(\theta_{k'})$  is the Wigner's  $d$ -function [63], and the spin basis  $\chi_{\sigma_{\Lambda'}}$  satisfies  $\hat{s}_z \chi_{\sigma_{\Lambda'}} = \sigma_{\Lambda'} \chi_{\sigma_{\Lambda'}}$  with corresponding spin operator in the  $z$ -direction  $\hat{s}_z$  and eigenvalue  $\sigma_{\Lambda'} = \pm 1, 0$ . The delta function  $\delta(k'_\perp - p'_\perp)$  with the phase factor  $e^{i(m'_n - \sigma_{\Lambda'})\varphi_{k'}}$  indicates that we have obtained the amplitude of a Bessel vortex state [2], which is represented by a cone with a spiral phase and a fixed angle  $\theta_{k'}$  in the momentum space (see Fig. 1). The vortex nature of the emitted photon could be seen more clearly if one transforms to the position space:

$$\mathcal{A}_{\omega',\Lambda'}(\mathbf{x}) = \frac{\mathcal{N}_{\text{NCS}}}{\sqrt{2\pi}\omega} e^{ik'_z z} \sum_{n,\sigma_{\Lambda'}} (-1)^{m'_n} i^{(m'_n - \sigma_{\Lambda'})} d^1_{\sigma_{\Lambda'},\Lambda'}(\theta_{k'}) \times e^{i(m'_n - \sigma_{\Lambda'})\varphi_r} J_{m'_n - \sigma_{\Lambda'}}(k'_\perp r) \chi_{\sigma_{\Lambda'}} \mathcal{M}_n(s_0), \quad (3)$$

where  $\{r, \varphi_r, z\}$  form cylindrical coordinates. Acting the TAM operator  $\hat{J}_z = \hat{s}_z + \hat{L}_z$  (OAM operator  $\hat{L}_z = -i\frac{\partial}{\partial\varphi_r}$ ) on Eq. (3), one finds that  $m'_n$  is the TAM number along  $z$  axis carried by the  $\gamma$  photon for a fixed harmonic  $n$  [2, 24]. The phase factor  $e^{i(m'_n - \sigma_{\Lambda'})\varphi_r}$  encodes two kinds of spin-orbit-interactions (SOI): one is the intrinsic SOI of a vortex light [64] causing its OAM number  $l'_n$  to take three values  $\{m'_n - \Lambda', m'_n, m'_n + \Lambda'\}$  [24, 52]; the other is SOI during NCS where SAM of electrons and laser photons contribute to the emitted photon OAM. For ultrarelativistic incoming electrons, the radiation

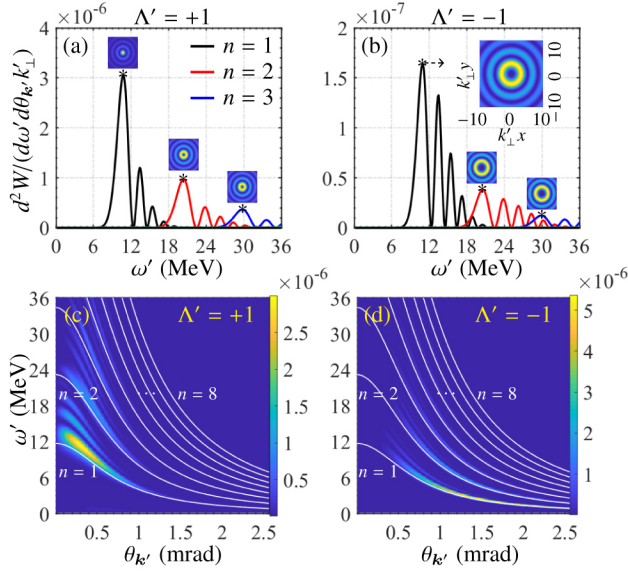


FIG. 2. Upper panels: radiation rates for the vortex  $\gamma$  photons with  $\theta_{k'} \approx 0.35$  mrad for the first 3 harmonics for helicities (a)  $\Lambda' = +1$  and (b)  $\Lambda' = -1$ ; Inset: the transverse intensity distributions given in arbitrary units calculated from  $|\mathbf{A}_{\omega'}(\mathbf{x})|^2$  for  $\omega'$  taken at main harmonic peaks marked by asterisks. Lower panels: the angle-resolved energy spectra in Eq. (4) for photon helicities (c)  $\Lambda' = +1$  and (d)  $\Lambda' = -1$ ; white lines stand for kinematic relations for harmonics  $\omega'_n(\theta_{k'})$  in monochromatic fields.

angle is estimated as  $\theta_{k'} \sim \frac{1}{\gamma_0} \ll 1$  with the electron relativistic factor  $\gamma_0 = \frac{\varepsilon}{m_e}$ , and the Wigner function  $d^1_{\sigma_{\Lambda'}, \Lambda'}(\theta_{k'})$  for small angles indicates that  $\sigma_{\Lambda'} = \Lambda'$  dominates and  $l'_n = m'_n - \Lambda'$ . As the electron spin-flip channel ( $\lambda \neq \lambda'$ ) is negligible in NCS under moderate laser intensities ( $\xi \sim 1$ ), one gets  $m'_n = n$ . Therefore,  $\gamma$  photon from the  $n$ -th harmonic of NCS corresponds to the vortex mode with SAM  $\Lambda'$  and OAM  $l'_n = n - \Lambda'$ , which is consistent with the existing results for the radiation of charged particles [47–49].

To obtain the photon radiation rate, one has to choose a specific detector basis. As optical techniques are blind to the vortex structure of a  $\gamma$  photon, the “detector” could be an angular momentum sensitive atomic or nuclear system [28]. After projecting the wave function of the emitted  $\gamma$  photon onto vortex eigenmodes, the  $S$ -matrix element for the vortex photon generation could be written in terms of the harmonic amplitude in Eq.(1). As a result, the probability for the vortex photon emission is written as [59]:

$$\frac{d^2 W_{\text{vortex}}}{d\omega' d\theta_{k'}} = \frac{e^2 k'_\perp}{(kp)(kp')} \sum_n \delta_{m'_n, n+\lambda-\lambda'} |\mathcal{M}_n(s)|^2, \quad (4)$$

where  $k'_\perp = \omega' \sin \theta_{k'}$  and  $\delta_{m'_n, n+\lambda-\lambda'}$  indicates the TAM conservation along the collision axis. The  $\delta$ -function wipes out the interference between different harmonics as a consequence of recording the radiation as vortex photons with definite TAM. Thus, the radiation rate is an incoherent sum over harmonics, and each harmonic represents a vortex state with definite TAM number  $m'_n = n$ .

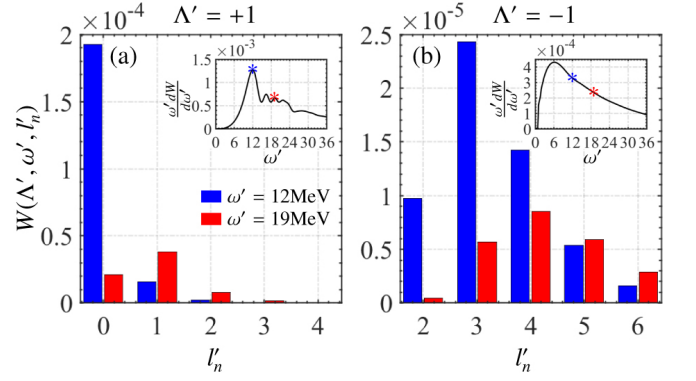


FIG. 3. The OAM distributions of incoherent vortex  $\gamma$  photons with energies  $\omega' = 12$  MeV and  $\omega' = 19$  MeV for helicities (a)  $\Lambda' = +1$  and (b)  $\Lambda' = -1$ . Inset: the power spectra of the emitted polarized photons  $\frac{\omega' dW}{d\omega'}$  where two energies marked by asterisks with same colors as in the OAM distributions. Note, OAM values start from  $l'_1 = 0$  for  $\Lambda' = +1$  and  $l'_1 = 2$  for  $\Lambda' = -1$  because of  $l'_n = n - \Lambda'$ .

The above analytical results hold for optical lasers with the pulse duration  $\tau \gtrsim 20$  fs regardless of the electron energy and the laser intensity as long as the single photon emission along the collision axis is dominated. In the following, we present numerical results where we assume the electron energy  $\varepsilon = 1$  GeV, the laser intensity  $\xi = 1$ , the central laser photon energy  $\omega = 1.55$  eV and the temporal pulse shape  $g(\phi) = \cos^2(\frac{\phi}{2N_{\text{cycle}}})$  with  $N_{\text{cycle}} = 10$  (corresponding to an optical laser with  $\lambda_0 \approx 0.8 \mu\text{m}$ ,  $I \approx 2 \times 10^{18}$  W/cm<sup>2</sup> and  $\tau \approx 26.7$  fs). Figure 2 shows the radiation rates of polarized vortex  $\gamma$  photons calculated via Eq. (4). As is identified from Eq. (2), the vortex  $\gamma$  photon to be absorbed by the nuclear or atomic system is in a coherent state with definite  $\theta_{k'}$ , hence we present the energy spectra for a fixed angle in Figs. 2 (a) and (b). The  $n$ -th harmonic corresponds to the vortex state with TAM number  $m'_n = n$  and OAM number  $l'_n = n - \Lambda'$ . The transversal distributions for  $|\mathbf{A}_{\omega'}(\mathbf{x})|^2$  in the inset feature the doughnut shape of the photon with nonzero OAM. Moreover, the ponderomotive broadening due to the finite pulse shape would cause the nearby harmonics to overlap [58], and one could find multiple OAM modes for certain energy and polarization. This feature holds for a wide range of  $\theta_{k'}$  as seen from the angle-resolved spectra given in Figs. 2 (c) and (d), where the white lines stand for the kinematic relation for the monochromatic laser. Each group of coordinates  $(\Lambda', \omega', \theta_{k'})$  represents an independent radiation event and defines a coherent vortex state with fixed OAM.

Since vortex photons formed from radiations with different  $\theta_{k'}$  overlap in the transverse position space, we introduce an incoherent summation over  $\theta_{k'}$  in Eq. (4) and obtain  $\frac{dW_{\text{vortex}}}{d\omega' d\theta_{k'}} \equiv \sum_n W(\Lambda', \omega', l'_n)$ , where we have shift from  $m'_n$  to  $l'_n$  for the convenience of discussing OAM. We then observe that  $\gamma$  photons with the definite energy and polarization  $(\Lambda', \omega')$  (see two asterisks in the inset of Fig 3) can be identified as a mixed state of vortex  $\gamma$  photons with different OAM numbers (see OAM distributions in Fig 3). This could be explained as follows. All laser photons contributing to NCS carry one unit of SAM, while their energies differ from the central laser

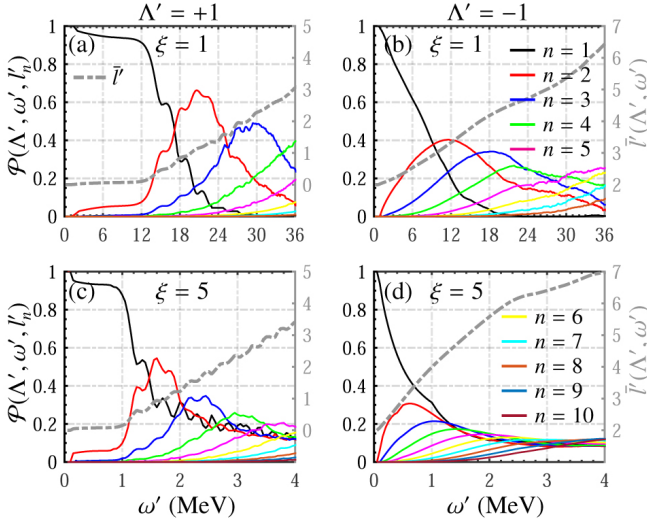


FIG. 4. The OAM ratios  $\mathcal{P}(\Lambda', \omega', l'_n)$  over energy spectra for polarized vortex  $\gamma$  photons. Results are presented up to the 10-th harmonic (the solid lines) and corresponding OAM values are implied via  $l'_n = n - \Lambda'$ . The average OAM number  $\bar{l}'(\Lambda', \omega')$  is given by the gray dashed line.

photon energy  $\omega$  due to the finite temporal pulse shape, thus, the radiated  $\gamma$  photon with certain energy  $\omega'$  could be the result of various multiphoton absorption events, and each event results in the same energy  $\omega'$  but with different number of laser photons involved. In addition, if we define the polarization degree for each harmonic as  $P_n(\omega') = \frac{W(\Lambda'=+1, \omega', n) - W(\Lambda'=-1, \omega', n)}{|W(\Lambda'=+1, \omega', n) + W(\Lambda'=-1, \omega', n)|}$ , we get for the polarized vortex  $\gamma$  photon with  $\omega' = 12$  MeV  $P_1 \approx 90.37\%$ ,  $P_2 \approx -23.44\%$ ,  $P_3 \approx -74.16\%$ , etc., which are different from the result for the plane wave  $\gamma$  photon  $P(\omega' = 12\text{MeV}) \approx 58.95\%$  (in the latter, all harmonics are counted into). We stress that such incoherent nature of the generated vortex photon is the crucial feature of strong laser-based  $\gamma$  ray sources. This new recognition of vortex  $\gamma$  photons in turn calls for novel considerations with regard to its applications in nuclear or particle physics studies, in which the current assumption is that the available vortex particles are in a pure coherent state [9, 10, 24].

Now we analyze the OAM property of the  $\gamma$  photon beam over the whole energy range. We introduce the ratios of polarized vortex photons with OAM in the overall incoherent beam as:

$$\mathcal{P}(\Lambda', \omega', l'_n) = \frac{W(\Lambda', \omega', l'_n)}{\sum_n W(\Lambda', \omega', l'_n)}. \quad (5)$$

Corresponding numerical results are given in Fig. 4 for laser intensities  $\xi = 1$  and  $\xi = 5$  ( $I \approx 5 \times 10^{19}$  W/cm<sup>2</sup>) and other parameters are the same as those in Fig. 2. At low energy regimes below the Compton edge, the first harmonic dominates the radiation, thus the corresponding  $\gamma$  photons carry nonzero OAM only for  $\Lambda' = -1$  due to the relation  $l'_1 = 1 - \Lambda'$ . As the energy increases, the appearance of the peak in each harmonic indicates the dominance of the corresponding OAM mode [see Figs. 4 (a) and (b)]. However, when the laser intensity increases, the feature is only weakly

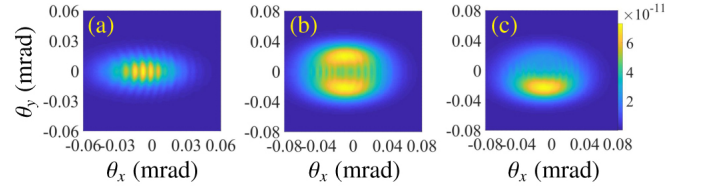


FIG. 5. The angular distributions  $\frac{dW}{d\Omega}$  of electrons from NLBW scattering of vortex  $\gamma$  photons in a linearly polarized laser pulse. The colliding  $\gamma$  photons are in the (a) plane wave, (b) vortex eigenstate and (c) vortex superposition state.

preserved for  $\Lambda' = +1$  [see Fig. 4 (c)]. We introduce the average intrinsic OAM at certain energy and polarization defined as  $\bar{l}'(\Lambda', \omega') = \sum_n \mathcal{P}(\Lambda', \omega', l'_n) l'_n$ . We find that the average OAM carried by  $\gamma$  photons gradually increases as the energy becomes large since more harmonics contribute, while the lower harmonics are also present due to the ponderomotive broadening caused by the finite temporal shape. This feature is different from the monochromatic results, in which the lower harmonics will not affect the higher harmonic region and the  $\bar{l}'$  line exhibits a staircase pattern [59]. Our results indicate that the  $\gamma$  photons radiated in a CP laser possess intrinsic OAM inherited from SAM of absorbed laser photons. This is missing in previous studies [39–46], in which SAM and OAM of the laser photons transfer wholly to the mechanical OAM of the final  $\gamma$  photon and electron. Such differences in understanding the angular momentum transfer relation during NCS need to be resolved, especially when the single photon emission is dominated as is assumed in this study. Those are most likely relevant for the intermediate regime ( $0.1 \lesssim \xi \lesssim 10$ ) which is currently under investigation [65, 66] and available for future experiments [55].

Having recognized the generation of vortex  $\gamma$  photons in intense lasers, we further explore strong-field QED processes for a possible detection of the vortex  $\gamma$  photon. Here, we consider NLBW scattering of the vortex  $\gamma$  photon in an intense laser where the incoming  $\gamma$  photon is generated from NCS. Since no OAM-sensitive “detector” is present to project the  $\gamma$  photon onto a specific OAM mode, the general phase structure indicated by Eq. (2) is kept. Assuming the outgoing particles to be plane waves, the differential rate for the vortex photon scattering can be written as the following incoherent sum [59],

$$\frac{dW_{\text{vortex}}}{d\Omega} = \int \frac{d\varphi_{\mathbf{k}'}}{2\pi} F(\varphi_{\mathbf{k}'}) \frac{dW_{\text{pw}}(\theta_{\mathbf{k}'}, \varphi_{\mathbf{k}'})}{d\Omega}, \quad (6)$$

where  $F(\varphi_{\mathbf{k}'}) = |C_1|^2 + |C_2|^2 + 2|C_1||C_2|\cos(\Delta m(\varphi_{\mathbf{k}'} - \frac{\pi}{2}) + \delta)$ ,  $\frac{dW_{\text{pw}}}{d\Omega}$  is the usual NLBW scattering rate for an incoming plane wave photon. For an illustrative example, we set the energy of the vortex  $\gamma$  photon  $\omega' = 14$  GeV, the cone angle  $\theta_{\mathbf{k}'} \approx 0.027$  mrad, and the temporal envelope  $g(\phi) = \sin^4(\frac{\phi}{2N_{\text{cycle}}})$  with  $N_{\text{cycle}} = 5$  and intensity  $\xi = 1$ . We consider pair creations of the  $\gamma$  photons in the TAM eigenmode and the vortex superposition state, which could be generated from a single harmonic and from overlapping of different harmonics of NCS, respectively. The NLBW scattering results for the former is calculated by setting  $F(\varphi_{\mathbf{k}'}) = 1$ , and the latter by setting  $C_{1,2} = \mathcal{M}_{n_1, n_2}(s)$ ,



$\Delta m = m_{n_1} - m_{n_2} = 1$  and  $\delta = 0$  for a symmetric laser pulse. As is shown in Fig. 5, the differential rate changes drastically due to different phase structures of the vortex  $\gamma$  photons. Therefore, the phase vorticity of the vortex  $\gamma$  photon is detectable in current experiments by measuring the angular distribution of the created electrons [67, 68], and this signature can be improved by adjusting the laser parameters, .e.g., intensity, pulse duration and pulse shape. Note that such a feature is unavailable in the linear Compton scattering, where the cone angle of the vortex photon is required to be orders of magnitude larger ( $\theta_{k'} \sim 10 - 100$  mrad) [16].

In conclusion, we investigated the generation of vortex  $\gamma$  photons in a CP laser pulse in the Furry picture of strong-field QED. We showed that,  $\gamma$  photons corresponding to NCS harmonics are described by vortex modes with intrinsic OAM as a result of spin-to-orbital angular momentum transfer during multiphoton absorption. However, due to the finite shape of the intense laser pulse, the generated  $\gamma$  photons are in general in the incoherent mixed state of various vortex modes. Furthermore,

the attained OAM is determined by the laser photon absorption number, and to obtain high OAM  $\gamma$  photons one may need to utilize OAM of vortex state electrons [69, 70] and/or vortex lasers. Finally, vortex  $\gamma$  photons may unveil new possibilities in strong-field QED studies, besides their already envisioned applications in nuclear and particle physics related researches.

*Acknowledgment:* We thank C. H. Keitel, K. Z. Hatsagortsyan, P. Zhang and I. P. Ivanov for helpful discussions. This work is supported by the National Natural Science Foundation of China (Grants Nos. 11874295, 12022506, U2267204, 11905169, 12275209, 12147176, 12135001, 11825502, 11921006 and U2241281), the Open Fund of the State Key Laboratory of High Field Laser Physics (Shanghai Institute of Optics and Fine Mechanics), the foundation of science and technology on plasma physics laboratory (No. JCKYS2021212008), and Open Foundation of Key Laboratory of High Power Laser and Physics, Chinese Academy of Sciences (SGKF202101).

- 
- [1] L. Allen, M. W. Beijersbergen, and R. Spreeuw *et al.*, Orbital angular momentum of light and the transformation of Laguerre-Gaussian laser modes, *Phys. Rev. A* **45**, 8185 (1992).
  - [2] B. A. Knyazev and V. Serbo, Beams of photons with nonzero projections of orbital angular momenta: new results, *Phys. Usp.* **61**, 449 (2018).
  - [3] H. He, M. Friese, and N. Heckenberg *et al.*, Direct observation of transfer of angular momentum to absorptive particles from a laser beam with a phase singularity, *Phys. Rev. Lett.* **75**, 826 (1995).
  - [4] V. Garcés-Chávez, D. McGloin, and M. Padgett *et al.*, Observation of the transfer of the local angular momentum density of a multiringed light beam to an optically trapped particle, *Phys. Rev. Lett.* **91**, 093602 (2003).
  - [5] A. Mair, A. Vaziri, and G. Weihs *et al.*, Entanglement of the orbital angular momentum states of photons, *Nature* **412**, 313 (2001).
  - [6] J. Leach, B. Jack, and J. Romero *et al.*, Violation of a bell inequality in two-dimensional orbital angular momentum state-spaces, *Opt. Express* **17**, 8287 (2009).
  - [7] G. A. Swartzlander, Peering into darkness with a vortex spatial filter, *Opt. Lett.* **26**, 497 (2001).
  - [8] G. A. Swartzlander, E. L. Ford, and R. S. Abdul-Malik *et al.*, Astronomical demonstration of an optical vortex coronagraph, *Opt. Express* **16**, 10200 (2008).
  - [9] I. P. Ivanov, N. Korchagin, A. Pimikov, and P. Zhang, Doing spin physics with unpolarized particles, *Phys. Rev. Lett.* **124**, 192001 (2020).
  - [10] I. P. Ivanov, Promises and challenges of high-energy vortex states collisions, *Prog. Part. Nucl. Phys.* **127**, 103987 (2022).
  - [11] M. Durante, P. Indicato, B. Jonson, and V. Koch *et al.*, All the fun of the FAIR: fundamental physics at the facility for antiproton and ion research, *Phys. Scripta* **94**, 033001 (2019).
  - [12] M. W. Krasny, The gamma factory proposal for CERN, arXiv:1511.07794.
  - [13] D. Budker, J. R. Crespo López-Urrutia, and A. Derevianko *et al.*, Atomic physics studies at the Gamma Factory at CERN, *Annalen Phys.* **532**, 2000204 (2020).
  - [14] D. Budker, M. Gorchtein, and A. Surzhykov *et al.*, Expanding nuclear physics horizons with the Gamma Factory, *Annalen Phys.* **534**, 2100284 (2021).
  - [15] R. Aboushelbaya, K. Glize, and A. F. Savin *et al.*, Orbital angular momentum coupling in elastic photon-photon scattering, *Phys. Rev. Lett.* **123**, 113604 (2019).
  - [16] J. A. Sherwin, Compton scattering of Bessel light with large recoil parameter, *Phys. Rev. A* **96**, 062120 (2017).
  - [17] S.-H. Lei, Z.-G. Bu, and W.-Q. Wang *et al.*, Generation of relativistic positrons carrying intrinsic orbital angular momentum, *Phys. Rev. D* **104**, 076025 (2021).
  - [18] Z.-G. Bu, L.-L. Ji, and S.-H. Lei *et al.*, Twisted Breit-Wheeler electron-positron pair creation via vortex gamma photons, *Phys. Rev. Res.* **3**, 043159 (2021).
  - [19] Y.-J. Shen, X.-J. Wang, and Z.-W. Xie *et al.*, Optical vortices 30 years on: OAM manipulation from topological charge to multiple singularities, *Light: Sci. Appl.* **8**, 1 (2019).
  - [20] A. G. Peele, P. J. McMahon, and D. Paterson *et al.*, Observation of an X-ray vortex, *Opt. Lett.* **27**, 1752 (2002).
  - [21] B. Terhalle, A. Langner, and B. Päivänranta *et al.*, Generation of extreme ultraviolet vortex beams using computer generated holograms, *Opt. Lett.* **36**, 4143 (2011).
  - [22] G. Gariepy, J. Leach, and K. T. Kim *et al.*, Creating high-harmonic beams with controlled orbital angular momentum, *Phys. Rev. Lett.* **113**, 153901 (2014).
  - [23] E. Hemsing, A. Knyazik, and M. Dunning *et al.*, Coherent optical vortices from relativistic electron beams, *Nat. Phys.* **9**, 549 (2013).
  - [24] U. D. Jentschura and V. G. Serbo, Generation of high-energy photons with large orbital angular momentum by Compton backscattering, *Phys. Rev. Lett.* **106**, 013001 (2011).
  - [25] V. Petrillo, G. Dattoli, I. Drebot, and F. Nguyen, Compton scattered X-Gamma rays with orbital momentum, *Phys. Rev. Lett.* **117**, 123903 (2016).
  - [26] Y. Taira, T. Hayakawa, and M. Katoh, Gamma-ray vortices from nonlinear inverse Thomson scattering of circularly polarized light, *Sci. Rep.* **7**, 1 (2017).
  - [27] Y.-Y. Chen, K. Z. Hatsagortsyan, and C. H. Keitel, Generation of twisted  $\gamma$ -ray radiation by nonlinear Thomson scattering of twisted light, *Matter Radiat. Extremes* **4**, 024401 (2019).

- [28] O. V. Bogdanov, P. Kazinski, and G. Y. Lazarenko, Semiclassical probability of radiation of twisted photons in the ultrarelativistic limit, *Phys. Rev. D* **99**, 116016 (2019).
- [29] C. N. Danson, C. Haefner, and J. Bromage *et al.*, Petawatt and exawatt class lasers worldwide, *High Power Laser Sci. Eng.* **7**, e54 (2019).
- [30] J. W. Yoon, C. Jeon, and J. Shin *et al.*, Achieving the laser intensity of  $5.5 \times 10^{22}$  W/cm<sup>2</sup> with a wavefront-corrected multi-PW laser, *Opt. Express* **27**, 20412 (2019).
- [31] J. W. Yoon, Y. G. Kim, I. W. Choi, J. H. Sung, H. W. Lee, S. K. Lee, and C. H. Nam, Realization of laser intensity over  $10^{23}$  W/cm<sup>2</sup>, *Optica* **8**, 630 (2021).
- [32] S. Chen, N. Powers, and I. Ghebregziabher *et al.*, MeV-energy X rays from inverse Compton scattering with laser-wakefield accelerated electrons, *Phys. Rev. Lett.* **110**, 155003 (2013).
- [33] G. Sarri, D. Corvan, and W. Schumaker *et al.*, Ultrahigh brilliance multi-MeV  $\gamma$ -ray beams from nonlinear relativistic Thomson scattering, *Phys. Rev. Lett.* **113**, 224801 (2014).
- [34] J. Cole, K. Behm, and E. Gerstmayr *et al.*, Experimental evidence of radiation reaction in the collision of a high-intensity laser pulse with a laser-wakefield accelerated electron beam, *Phys. Rev. X* **8**, 011020 (2018).
- [35] K. Poder, M. Tamburini, and G. Sarri *et al.*, Experimental signatures of the quantum nature of radiation reaction in the field of an ultraintense laser, *Phys. Rev. X* **8**, 031004 (2018).
- [36] Y.-F. Li, R. Shaisultanov, Y.-Y. Chen, and F. Wan *et al.*, Polarized ultrashort brilliant multi-gev  $\gamma$  rays via single-shot laser-electron interaction, *Phys. Rev. Lett.* **124**, 014801 (2020).
- [37] S. Tang, B. King, and H. Hu, Highly polarised gamma photons from electron-laser collisions, *Phys. Lett. B* **809**, 135701 (2020).
- [38] Y. Wang, M. Ababekri, and F. Wan *et al.*, Brilliant circularly polarized  $\gamma$ -ray sources via single-shot laser plasma interaction, *Opt. Lett.* **47**, 3355 (2022).
- [39] C. Liu, B.-F. Shen, and X.-M. Zhang *et al.*, Generation of gamma-ray beam with orbital angular momentum in the QED regime, *Phys. Plasmas* **23**, 093120 (2016).
- [40] Y.-Y. Chen, J.-X. Li, K. Z. Hatsagortsyan, and C. H. Keitel,  $\gamma$ -Ray Beams with Large Orbital Angular Momentum via Nonlinear Compton Scattering with Radiation Reaction, *Phys. Rev. Lett.* **121**, 074801 (2018).
- [41] Z. Gong, R. Hu, H. Lu, and J. Yu *et al.*, Brilliant GeV Gamma-ray flash from inverse Compton scattering in the QED regime, *Plasma Phys. Control. Fusion* **60**, 044004 (2018).
- [42] Y.-Y. Liu, Y. I. Salamin, and Z.-K. Dou *et al.*, Vortex  $\gamma$  rays from scattering laser bullets off ultrarelativistic electrons, *Opt. Lett.* **45**, 395 (2020).
- [43] J. Wang, X. Li, and L. Gan *et al.*, Generation of intense vortex gamma rays via spin-to-orbital conversion of angular momentum in relativistic laser-plasma interactions, *Phys. Rev. Applied* **14**, 014094 (2020).
- [44] Y.-T. Hu, J. Zhao, H. Zhang, and Y. Lu *et al.*, Attosecond  $\gamma$ -ray vortex generation in near-critical-density plasma driven by twisted laser pulses, *Appl. Phys. Lett.* **118**, 054101 (2021).
- [45] H. Zhang, J. Zhao, and Y. Hu *et al.*, Efficient bright  $\gamma$ -ray vortex emission from a laser-illuminated light-fan-in-channel target, *High Power Laser Sci. Eng.* **9**, 11 (2021).
- [46] M. A. Bake, T. Suo, and X. Baisong, Bright  $\gamma$ -ray source with large orbital angular momentum from the laser near-critical-plasma interaction, *Plasma Sci. and Technol.* **24**, 095001 (2022).
- [47] S. Sasaki and I. McNulty, Proposal for generating brilliant X-ray beams carrying orbital angular momentum, *Phys. Rev. Lett.* **100**, 124801 (2008).
- [48] J. Bahrdt, K. Holldack, and P. Kuske *et al.*, First observation of photons carrying orbital angular momentum in undulator radiation, *Phys. Rev. Lett.* **111**, 034801 (2013).
- [49] M. Katoh, M. Fujimoto, and H. Kawaguchi *et al.*, Angular momentum of twisted radiation from an electron in spiral motion, *Phys. Rev. Lett.* **118**, 094801 (2017).
- [50] D. Karlovets, G. Geloni, G. Sizykh, and V. Serbo, Generation of vortex particles via generalized measurements, arXiv:2201.07997.
- [51] F. Mackenroth and A. Di Piazza, Nonlinear Compton scattering in ultrashort laser pulses, *Phys. Rev. A* **83**, 032106 (2011).
- [52] U. D. Jentschura and V. G. Serbo, Compton upconversion of twisted photons: backscattering of particles with non-planar wave functions, *Eur. Phys. J. C* **71**, 1 (2011).
- [53] A. Gonoskov, T. Blackburn, M. Marklund, and S. Bulanov, Charged particle motion and radiation in strong electromagnetic fields, *Rev. Mod. Phys.* **94**, 045001 (2022).
- [54] A. Fedotov, A. Ilderton, and F. Karbstein *et al.*, Advances in QED with intense background fields, arXiv:2203.00019.
- [55] H. Abramowicz, U. Acosta, and A. *et al.*, Conceptual design report for the LUXE experiment, *Eur. Phys. J. ST* **230**, 2445 (2021).
- [56] F. Salgado, N. Cavanagh, and T. *et al.*, Single particle detection system for strong-field QED experiments, *New J. Phys.* **24**, 015002 (2021).
- [57] S. Meuren, P. H. Bucksbaum, and N. J. Fisch *et al.*, On seminal HEDP research opportunities enabled by colocating multi-petawatt laser with high-density electron beams, arXiv:2002.10051.
- [58] D. Seipt, V. Kharin, and S. Rykovanov *et al.*, Analytical results for nonlinear Compton scattering in short intense laser pulses, *J. Plasma Phys.* **82**, 655820203 (2016).
- [59] See the supplemental materials for the details of derivations of the  $S$ -matrix element, the photon wave function, the radiation rate and numerical results for the monochromatic laser.
- [60] V. B. Berestetskii, E. M. Lifshitz, and L. P. Pitaevskii, *Quantum Electrodynamics* (Pergamon Press, 1982).
- [61] I. P. Ivanov, Creation of two vortex-entangled beams in a vortex-beam collision with a plane wave, *Phys. Rev. A* **85**, 033813 (2012).
- [62] R. Van Boxem, B. Partoens, and J. Verbeeck, Inelastic electron-vortex-beam scattering, *Phys. Rev. A* **91**, 032703 (2015).
- [63] D. A. Varshalovich, A. N. Moskalev, and V. K. Khersonskii, *Quantum theory of angular momentum* (World Scientific, 1988).
- [64] K. Bliokh, F. Rodríguez-Fortuñ, F. Nori, and A. Zayats, Spin-orbit interactions of light, *Nat. Photonics* **9**, 796 (2015).
- [65] A. Di Piazza, M. Tamburini, S. Meuren, and C. H. Keitel, Improved local-constant-field approximation for strong-field QED codes, *Phys. Rev. A* **99**, 022125 (2019).
- [66] T. Blackburn, A. MacLeod, and B. King, From local to nonlocal: higher fidelity simulations of photon emission in intense laser pulses, *New J. Phys.* **23**, 085008 (2021).
- [67] B. Wolter, M. G. Pullen, and A.-T. Le *et al.*, Ultrafast electron diffraction imaging of bond breaking in di-ionized acetylene, *Science* **354**, 308 (2016).
- [68] W.-T. Wang, K. Feng, and L.-T. Ke *et al.*, Free-electron lasing at 27 nanometres based on a laser wakefield accelerator, *Nature* **595**, 516 (2021).
- [69] S. Lloyd, M. Babiker, G. Thirunavukkarasu, and J. Yuan, Electron vortices: Beams with orbital angular momentum, *Rev. Mod. Phys.* **89**, 035004 (2017).
- [70] K. Y. Bliokh, I. P. Ivanov, and G. Guzzinati *et al.*, Theory and applications of free-electron vortex states, *Phys. Rep.* **690**, 1 (2017).